Article:

Ellis, M.O.A. orcid.org/0000-0003-0338-8920 and Chantrell, R.W. (2015) Switching times of nanoscale FePt: finite size effects on the linear reversal mechanism. Applied Physics Letters, 106 (16). 162407. ISSN 0003-6951

https://doi.org/10.1063/1.4919051

Applied Physics Letters

Switching times of nanoscale FePt: Finite size effects on the linear reversal mechanism

Cite as: Appl. Phys. Lett. **106**, 162407 (2015); https://doi.org/10.1063/1.4919051
Submitted: 09 February 2015 . Accepted: 14 April 2015 . Published Online: 22 April 2015

M. O. A. Ellis, and R. W. Chantrell

ARTICLES YOU MAY BE INTERESTED IN

The Curie temperature distribution of FePt granular magnetic recording media
Applied Physics Letters **101**, 052406 (2012); https://doi.org/10.1063/1.4740075

Review Article: FePt heat assisted magnetic recording media
Journal of Vacuum Science & Technology B **34**, 060801 (2016); https://doi.org/10.1116/1.4965980

The design and verification of MuMax3
AIP Advances **4**, 107133 (2014); https://doi.org/10.1063/1.4899186

Switching times of nanoscale FePt: Finite size effects on the linear reversal mechanism

M. O. A. Ellis and R. W. Chantrell
Department of Physics, University of York, York YO10 5DD, United Kingdom

(Received 9 February 2015; accepted 14 April 2015; published online 22 April 2015)

The linear reversal mechanism in FePt grains ranging from 2.316 nm to 5.404 nm has been simulated using atomistic spin dynamics, parametrized from *ab-initio* calculations. The Curie temperature and the critical temperature (T^*), at which the linear reversal mechanism occurs, are observed to decrease with system size whilst the temperature window $T^* < T < T_C$ increases. The reversal paths close to the Curie temperature have been calculated, showing that for decreasing system size the reversal path becomes more elliptic at lower temperatures, consistent with the decrease in the Curie temperature arising from finite size effects. Calculations of the minimum pulse duration show faster switching in small grains and are qualitatively described by the Landau-Lifshitz-Bloch equation with finite size atomistic parameterization, which suggests that multiscale modeling of FePt down to a grain size of ≈3.5 nm is possible. © *2015 AIP Publishing LLC*.
[http://dx.doi.org/10.1063/1.4919051]

The properties of $L1_0$ FePt are of paramount importance for the next generation of high density magnetic recording technology, in particular, Heat Assisted Magnetic Recording (HAMR). $L1_0$ FePt exhibits a very large uniaxial anisotropy of $K_u \approx 7 \times 10^6\,\mathrm{Jm^{-3}}$, which allows possible stable grain sizes down to a limit of around 3 nm.[1] To record data, the medium is heated close to or above the Curie temperature where the anisotropy is significantly reduced, therefore an understanding of the dynamical behavior of nanometer FePt grains at elevated temperatures is essential. In particular, at temperatures close to T_C, it has been shown that the magnetization reverses by a linear longitudinal route rather than a precessional one.[2,3] Using the Landau-Lifshitz-Bloch (LLB) model, Kazantseva *et al.*[2] predicted that the linear reversal regime occurs at a critical temperature T^* and derived a expression for the reversal time in this regime. Following this Barker *et al.*[3] observed the linear reversal mechanism using an atomistic model of FePt which agreed well with the LLB modeling. However, the question of linear reversal in finite nanometer grains and the size dependence of the switching properties remains open.

Here, an atomistic model is used to investigate the properties of nanometer grains from 2.316 nm to 5.404 nm at temperatures close to the Curie temperature. Using Langevin dynamics methods, we investigate the static and dynamic properties as a function of the grain size. We calculate the equilibrium magnetization and susceptibilities for each system size which allow us to parametrize the LLB model. Using this parametrization, we can then compare the reversal path ellipticity and times calculated using the atomistic model to those predicted by the LLB.

The properties of nanometer FePt particles have been investigated using *ab-initio* methods by Chepulskii and Butler.[4] Their calculations show that the magneto-crystalline anisotropy and magnetic moment vary significantly with system size and shape. However, the sizes considered are smaller than 1 nm so here we use the parameterization of bulk materials given by Mryasov *et al.*[5] The finite size effects in FePt have been investigated using a similar model by Lyberatos *et al.*[6] and Hovorka *et al.*[7] Lyberatos *et al.* have further investigated the grain size effects on the HAMR write process showing that smaller grain sizes require larger write fields.[8]

Atomistic spin models are increasingly used for dynamic magnetization calculations (Evans *et al.*[9]). The *ab-initio* simulations of Mryasov *et al.* show that the $L1_0$ FePt spin Hamiltonian can be written in the following form, involving only Fe degrees of freedom with parameters mediated by the Pt

$$\mathcal{H} = -\sum_{i \neq j} J_{ij}\mathbf{S}_i \cdot \mathbf{S}_j - \sum_i d_i^{(0)}(S_i^z)^2 - \sum_{i \neq j} d_{ij}^{(2)} S_i^z S_j^z. \quad (1)$$

The first term is the mediated exchange interaction, the second term a uniaxial anisotropy, and the third a two-ion anisotropy which represents an anisotropic exchange interaction. The sum j is over the atoms within the interaction range, which extends for approximately 5 unit cells. It is important to note that our model includes a significant finite size effect in that, as noted by Nowak *et al.*,[10] there is a loss of anisotropy at the surface due to the reduction of coordination which results in a reduction of the 2-ion anisotropy contribution. These finite size effects mean that the total anisotropy varies from $K_u = 8.3 \times 10^6\,\mathrm{Jm^{-3}}$ for a 4.632 nm particle to $K_u = 7.3 \times 10^6\,\mathrm{Jm^{-3}}$ for a 2.316 nm particle. The dipolar field was not included in the calculations as at temperatures close to T_C, it has negligible effect and is not important in the linear reversal mechanism.

The time evolution of the magnetic properties is calculated using the Langevin dynamic approach. The Landau-Lifshitz-Gilbert (LLG) equation for an atomic spin is

$$\frac{\partial \mathbf{S}_i}{\partial t} = \frac{-\gamma}{(1+\lambda^2)\mu_s}\mathbf{S}_i \times (\mathbf{H}_i + \lambda \mathbf{S}_i \times \mathbf{H}_i), \quad (2)$$

where $\gamma = 1.76 \times 10^{11}\,\mathrm{s^{-1}T^{-1}}$ is the gyromagnetic ratio, $\mu_s = 3.23\mu_B$ is the saturation magnetic moment of the combined Fe and Pt atoms, $\lambda = 0.1$ is the atomistic damping/coupling parameter, and $\mathbf{H}_i$ is the effective field acting on the

0003-6951/2015/106(16)/162407/4/$30.00

spin. For these parameters, the saturation magnetization is $M_s = 1.075 \times 10^6\,\mathrm{JT^{-1}m^{-3}}$. Temperature is introduced via a thermal noise term which is added to the effective field, $\mathbf{H}_i = -\partial\mathcal{H}/\partial\mathbf{S}_i + \boldsymbol{\xi}_i$. The thermal noise is a Gaussian stochastic process with the following mean and variance:[11]

$$\langle \xi_{i,\alpha}(t)\rangle = 0, \tag{3}$$

$$\langle \xi_{i,\alpha}(t)\xi_{j,\beta}(t')\rangle = \delta_{ij}\delta_{\alpha\beta}\delta(t-t')\frac{2\mu_s\lambda k_B T}{\gamma}, \tag{4}$$

where i, j refer to atom numbers, α, β are Cartesian coordinates, and t, t' are the times. The resulting stochastic LLG equation is numerically solved using the semi-implicit integration scheme[12,13] with a time step $\Delta t = 10^{-16}$ s which has been tested to show stability.

We first investigate the temperature dependence of the magnetization and the apparent Curie temperature. The results are shown in Figure 1 for a selection of system sizes. Clearly, the smaller systems have a reduced equilibrium magnetization at a given temperature, as expected as a result of reduced coordination at the surfaces. The apparent Curie temperature can be extracted from fitting $m(T) = (1 - T/T_C(L))^\beta$ to the magnetization curves.[6] The extracted T_C values are reduced significantly from the bulk and described well by finite system size scaling theory[7]

$$\frac{T_C^\infty - T_C}{T_C^\infty} = \left(\frac{L}{d_0}\right)^{-1/\nu}. \tag{5}$$

The inset in Figure 1 shows the fitting to obtain $T_C^\infty = 665$ K, $\nu = 0.85699$, $d_0 = 0.4039$ nm which agree well with Refs. 7 and 6 for the long range FePt Hamiltonian which we utilize.

The switching time at elevated temperatures is strongly affected by the reversal mechanism, which is determined by the ratio of longitudinal and transverse susceptibilities, $\tilde{\chi}_\parallel, \tilde{\chi}_\perp$. Consequently, we next investigate the ratio of susceptibilities and make a comparison with bulk properties using an expression for the free energy, in the absence of an externally applied field[15,16]

$$\frac{F}{M_s V} = \begin{cases} \dfrac{m_x^2 + m_y^2}{2\tilde{\chi}_\perp} + \dfrac{\left(m^2 - m_e^2\right)^2}{8 m_e^2 \tilde{\chi}_\parallel} & T < T_c \\ \dfrac{m_x^2 + m_y^2}{2\tilde{\chi}_\perp} + \dfrac{3}{20\tilde{\chi}_\parallel}\dfrac{T_C}{T - T_C} & \\ \quad \times \left(m^2 + \dfrac{5}{3}\dfrac{T - T_C}{T_C}\right)^2 & T > T_c, \end{cases} \tag{6}$$

where m is the reduced magnetization, m_e is the equilibrium magnetization, and $\tilde{\chi}_\parallel, \tilde{\chi}_\perp$ are, respectively, the reduced parallel and perpendicular susceptibilities. We note that Eq. (6) gives the free energy governing the behavior of the LLB equation derived in Ref. 15, which allows us to connect the current calculations to the LLB equation as will be shown later. From the free energy, we find the following expression for the orientation dependence of the magnetization length, $m(\theta)$, for a bulk material:

$$m(\theta) = m_e\left(1 - 2\frac{\tilde{\chi}_\parallel}{\tilde{\chi}_\perp}\sin^2(\theta)\right)^{\frac{1}{2}}. \tag{7}$$

Equation (7) gives an important relationship between the ellipticity parameter and the characteristic parameters of the LLB equation. Specifically, the ratio of the longitudinal and perpendicular susceptibility determines the ellipticity of the reversal path. Equation (7) predicts a critical temperature, T^*, corresponding to $\tilde{\chi}_\parallel(T^*)/\tilde{\chi}_\perp(T^*) = 1/2$, at which point the perpendicular magnetization vanishes. T^* is the critical temperature above which the magnetization will reverse through the linear switching mechanism. By calculating the equilibrium magnetization and susceptibilities for finite nanometer systems, Eqs. (6) and (7) can be parametrized. The longitudinal and transverse susceptibilities have been calculated as χ_z and $\chi_x + \chi_y$, respectively. The ratio $\tilde{\chi}_\parallel(T)/\tilde{\chi}_\perp(T)$ is shown in Fig. 2. The points show the susceptibilities from the atomistic simulations, while the solid lines

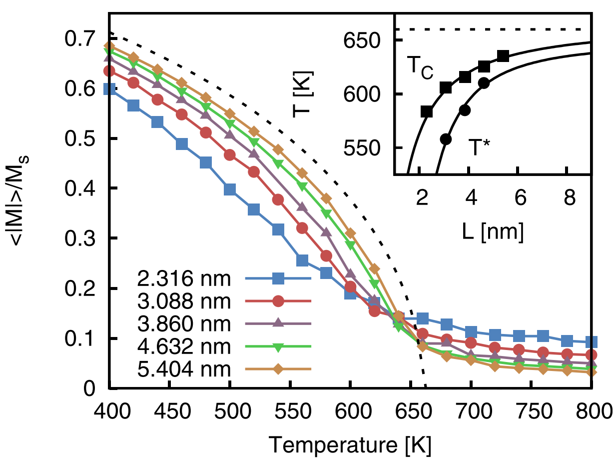

FIG. 1. The temperature dependence of the magnetization for particle sizes of 2.316 nm to 5.404 nm. The dashed black line shows the magnetization for a bulk system from Ref. 14 for comparison. As the system size decreases, the magnetization below the Curie temperature decreases while above it the magnetization increases. The inset shows the Curie temperatures which have been extracted from fitting and T^* extracted from Figure 2. The solid lines are Eq. (5) fitted to find the critical exponent.

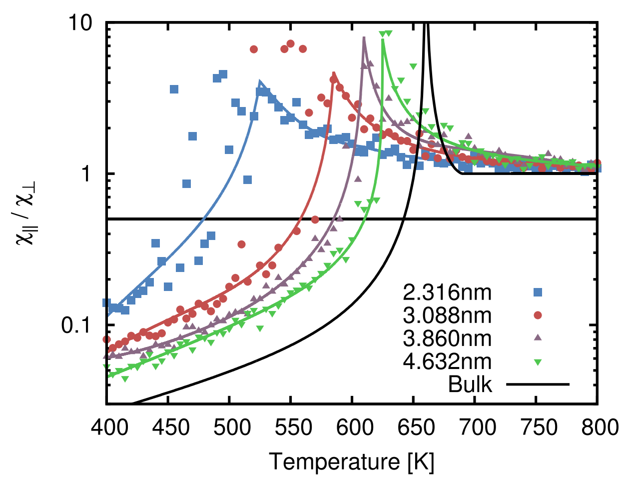

FIG. 2. The ratio of the parallel and perpendicular susceptibilities reaches a peak at different temperatures consistent with the Curie temperature extracted from the magnetization. The solid lines show functions that have been fitted the susceptibilities and the horizontal solid line gives $\tilde{\chi}_\parallel/\tilde{\chi}_\perp = 1/2$ defining the transition to linear reversal.

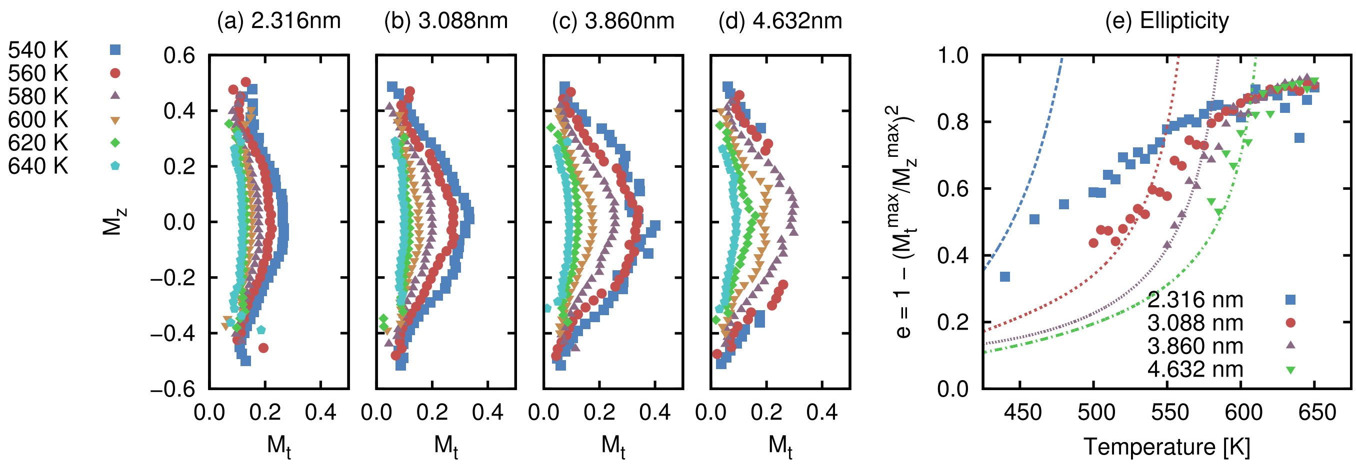

FIG. 3. The reversal paths of (a) 2.316 nm, (b) 3.088 nm, (c) 3.860 nm, and (d) 4.632 nm systems using a reversing field of 1 T. The reversal paths are calculated at different temperatures slightly below the Curie temperature. For the larger system sizes, the lower temperatures have not reversed with in the simulation time limit but as the system size decreases at the same temperature the system now reverses within the given time. (e) The ellipticity extracted from the reversal paths in (a)–(d) using Eq. (8). The dashed lines show the ellipticity that is expected by the LLB model using the finite size susceptibilities shown in Figure 2.

show a polynomial function that has been fitted to inverse susceptibilities individually in a similar manner to Ref. 14. The significant noise in the small grains arises from the thermal switching of the magnetization during the averaging of m_z leading to ergodicity breaking.[17] As the grain size decreases, the critical temperature T^* decreases and the apparent temperature window $T^* < T < T_C$ of the linear reversal region widens. T^* is shown in the inset of Fig. 1 alongside T_C which highlights the widening temperature window. Although the free energy expression given in Eq. (6) is strictly valid only for bulk systems, the temperature variation of $\tilde{\chi}_{\|}(T)/\tilde{\chi}_{\perp}(T)$ for all system sizes is consistent with the behavior shown by the reversal paths and the ellipticity.

Figures 3(a)–3(d) show the reversal paths for system size of 2.314 nm to 4.632 nm using a 1 T field to investigate the temperature dependence of the reversal path. In the 4.632 nm particle, the magnetization does not reverse within the simulation time limit of 400 ps for 540 K and 560 K but then there is a sharp transition to linear reversal, characterized by vanishing transverse magnetization, at 640 K. The smaller systems reverse at lower temperatures, but there is a less critical transition to the linear reversal path.

To further investigate the effect of the system size on the transition to the linear regime, we calculate the ellipticity of the reversal paths, defined as

$$e = 1 - \left(\frac{M_t^{\max}}{M_z^{\max}}\right)^2. \tag{8}$$

The ellipticity is shown in Figure 3(e) for the reversal paths shown in Figs. 3(a)–3(d). As discussed previously, the transition to the linear regime (where $e \approx 1$) occurs within a smaller temperature window for the larger systems. Also since the Curie temperature decreases for smaller system sizes, the window is centered at lower temperatures. The lines shown in Fig. 3(e) show the ellipticity from the LLB model which is $e_{\mathrm{LLB}} = 2\tilde{\chi}_{\|}(T)/\tilde{\chi}_{\perp}(T)$; this shows that the LLB model reasonably predicts the ellipticity but significant deviations occur for the smaller particles.

In terms of HAMR, the temperature dependence of the relaxation time is an important factor. It has been shown by Evans *et al.*[18] that the achievable recording density in HAMR is set by the equilibrium magnetization at the temperature at which the magnetization freezes. Consequently, it is vital to the HAMR process for the magnetization to be as close as possible to the equilibrium value at a given temperature, emphasizing the importance of the linear reversal mechanism and its associated fast switching time governed by longitudinal rather than transverse relaxation. As a measure of the relaxation time, we calculate the minimal pulse duration;[3] this is the time taken for m_z to first pass the $m_z = 0$ plane starting from an initial fully magnetized state. Figure 4 shows the minimal pulse duration calculated with a 1 T reversing field relevant to the HAMR process. The results show that there is a significant reduction in the relaxation time in small grains which arises from a convolution of two factors, the decrease of intrinsic properties and the transition from circular to linear reversal. The intrinsic parameters K and M_s both decrease with temperature and depend strongly on the system size. Since a large part of the anisotropy arises from the 2-ion

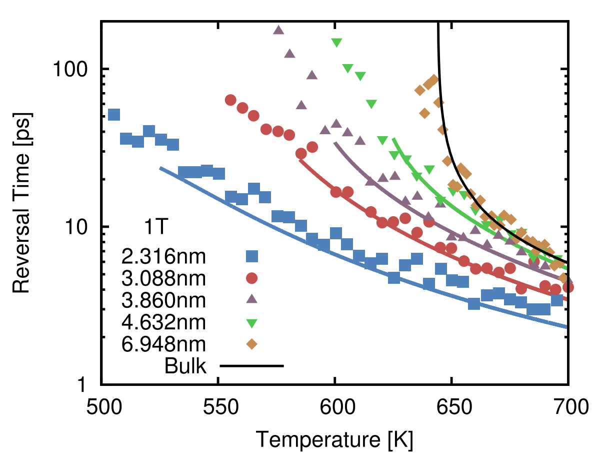

FIG. 4. The reversal time in a constant 1 T reversing field. The solid lines show the analytic minimum pulse duration which is derived in Ref. 2, the parameters for which are calculated from our atomistic simulations for the finite systems, while the black line is for bulk.

interaction, there is a strong decrease with grain size and thus the relaxation time predictable from the Arrhenius-Néel law.[19] In the elliptical and linear regimes, the free energy barrier is reduced significantly relative to the coherent reversal mechanism, leading to a further reduction of switching time with temperature over and above that predicted by the Arrhenius-Néel law. We note that both factors are essentially thermodynamic and emerge naturally from the atomistic model.

We compare these results to the expression for the minimum pulse duration derived from the LLB equation by Kazantseva *et al*.[2] The minimum pulse duration depends on the equilibrium magnetization and susceptibilities, so using the values already presented can be computed for each specific grain size, which are shown as solid lines in Figure 4. There is a good agreement but since the free energy assumes an infinite system, the problems arise at size dependent T_C so only the section above is shown. The analytic expression with finite input parameters shows qualitative agreement with the atomistic reversal times showing that for moderate system sizes, the LLB equation is applicable using parameters determined for the specific system size. The reversal times for the 6.948 nm particle are similar to the bulk LLB curve. For the smallest system sizes, the validity is questionable since it is far from the bulk regime in which the LLB is derived. However, for the sizes in excess of 3.5 nm potentially usable as HAMR media, the parameterization seems a practical proposition.

In summary, we have investigated the effects of finite size on the linear reversal regime of FePt which is of technological importance for HAMR. Atomistic calculations of the temperature dependence of the magnetization show that T_C decreases with decreasing system size as does the critical temperature for the linear reversal regime, T^*, determined from the susceptibilities. The transition to linear reversal also takes place at a lower temperature, with the temperature range of linear reversal increasing with decreasing size. The reversal characteristics have been calculated showing that the reversal paths do exhibit a trend towards linear reversal at T^* but in smaller grains the criticality of the transition is reduced. We find that the expression for the reversal time derived from the LLB equation gives switching times close to the atomistic results using values appropriate for each individual nanoparticle diameter. This suggests that a multiscale approach for HAMR media modeling is feasible using the LLB equation as a macrospin approximation to the behavior of nanoparticles, with parameters (equilibrium magnetization and susceptibilities) determined for each grain size. Given the importance of linear reversal to the HAMR process, this represents an important result for simulations of future generations of HAMR media as the grain size is inevitably reduced as linear densities increase.

The authors would like to thank A. Lyberatos for helpful discussions. Financial support from the Advanced Storage Technology Consortium was gratefully acknowledged.

[1]D. Weller, A. Moser, L. Folks, and M. Best, IEEE Trans. Magn. **36**, 10 (2000).
[2]N. Kazantseva, D. Hinzke, R. W. Chantrell, and U. Nowak, Europhys. Lett. **86**, 27006 (2009).
[3]J. Barker, R. F. L. Evans, R. W. Chantrell, D. Hinzke, and U. Nowak, Appl. Phys. Lett. **97**, 192504 (2010).
[4]R. V. Chepulskii and W. H. Butler, Appl. Phys. Lett. **100**, 142405 (2012).
[5]O. N. Mryasov, U. Nowak, R. W. Chantrell, and K. Y. Guslienko, Europhys. Lett. **69**, 805 (2005).
[6]A. Lyberatos, D. Weller, and G. J. Parker, J. Appl. Phys. **114**, 233904 (2013).
[7]O. Hovorka, S. Devos, Q. Coopman, W. J. Fan, C. J. Aas, R. F. L. Evans, and X. Chen, Appl. Phys. Lett. **101**, 052406 (2012).
[8]A. Lyberatos, D. Weller, and G. J. Parker, IEEE Trans. Magn. **50**, 1 (2014).
[9]R. F. L. Evans, W. J. Fan, P. Chureemart, T. A. Ostler, M. O. A. Ellis, and R. W. Chantrell, J. Phys.: Condens. Matter **26**, 103202 (2014).
[10]U. Nowak, O. Mryasov, R. Wieser, K. Guslienko, and R. Chantrell, Phys. Rev. B **72**, 172410 (2005).
[11]W. F. Brown, Phys. Rev. **130**, 1677 (1963).
[12]J. H. Mentink, M. V. Tretyakov, A. Fasolino, M. I. Katsnelson, and T. Rasing, J. Phys.: Condens. Matter **22**, 176001 (2010).
[13]M. O. A. Ellis, T. A. Ostler, and R. W. Chantrell, Phys. Rev. B **86**, 174418 (2012).
[14]N. Kazantseva, D. Hinzke, U. Nowak, R. W. Chantrell, U. Atxitia, and O. Chubykalo-Fesenko, Phys. Rev. B **77**, 184428 (2008).
[15]D. Garanin, Phys. Rev. B **55**, 3050 (1997).
[16]R. F. Evans, D. Hinzke, U. Atxitia, U. Nowak, R. Chantrell, and O. Chubykalo-Fesenko, Phys. Rev. B **85**, 014433 (2012).
[17]K. Binder, Rep. Prog. Phys. **60**, 487 (1997).
[18]R. F. L. Evans, R. W. Chantrell, U. Nowak, A. Lyberatos, and H.-J. Richter, Appl. Phys. Lett. **100**, 102402 (2012).
[19]L. Néel, Ann. Géophys. **5**, 99 (1949).